Joint Diseases and Related Surgery

Jt Dis Relat Surg
2026;37(3):822-837

ORIGINAL ARTICLE

Effects of BPC-157 and TB-500 on Achilles tendon healing in rats: A histopathological and biomechanical study

Ozancan Biçer, MD[1], Oktay Adanir, MD[1], Yiğit Güleryüz, MD[2], Emin Can Balci, MD[1], Yaşar Mahsut Dinçel, MD[3], Mehmet Yağız Yenigün, MD[1], Cemre Aydin, MD[1], Büşra Yaprak Bayrak, MD[4]

[1]Department of Orthopedics and Traumatology, Bağcılar Training and Research Hospital, İstanbul, Türkiye
[2]Department of Orthopedics and Traumatology, Beykoz State Hospital, İstanbul, Türkiye
[3]Department of Orthopedics and Traumatology, Tekirdağ Namık Kemal University Faculty of Medicine, Tekirdağ, Türkiye
[4]Department of Pathology, Kocaeli University Faculty of Medicine, Kocaeli, Türkiye

Tendons are composed primarily of type I collagen fibers embedded within a tenocyte-maintained extracellular matrix, a structure that provides high tensile strength but limited intrinsic regenerative capacity following injury. The Achilles tendon is the most frequently injured tendon in humans[1,2] and is particularly vulnerable to impaired healing because of its relatively poor vascular supply.[3-5] Consequently, healing is often characterized by prolonged remodeling, incomplete restoration of native tissue architecture, and inferior mechanical properties compared to uninjured tendon.[4]

The BPC-157 is a pentadecapeptide that has demonstrated proangiogenic and tissue-reparative effects in a variety of preclinical models.[6-9] In tendon-specific studies, BPC-157 improved

Received: May 04, 2026
Accepted: July 14, 2026
Published online: July 23, 2026

Correspondence: Oktay Adanir, MD. Bağcılar Eğitim ve Araştırma Hastanesi, Ortopedi ve Travmatoloji Kliniği, 34200 Bağcılar, İstanbul, Türkiye.

E-mail: droktayadanir@yahoo.com

Citation: Biçer O, Adanir O, Güleryüz Y, Balci EC, Dinçel YM, Yenigün MY, et al. Effects of BPC-157 and TB-500 on Achilles tendon healing in rats: A histopathological and biomechanical study. Jt Dis Relat Surg 2026;37(3):822-837. doi: 10.52312/jdrs.2026.2951.

© 2026 Joint Diseases and Related Surgery. This is an open access article published under the terms of the Creative Commons Attribution-NonCommercial 4.0 International License (CC BY-NC 4.0), which permits non-commercial use, distribution, reproduction, and adaptation in any medium, provided the original work is properly cited. http://creativecommons.org/licenses/by-nc/4.0/

ABSTRACT

Objectives: This study aims to evaluate the effects of BPC-157, synthetic thymosin beta-4 (TB-500), and their combination on Achilles tendon healing using biomechanical, histopathological, histochemical, and immunohistochemical analyses in a rat model.

Materials and methods: Thirty-two male Sprague-Dawley rats, each aged 12 weeks and weighing approximately 330 g, underwent standardized Achilles tendon transection and repair and were randomly assigned to four groups, with eight rats in each group: control, BPC-157 (10 μg/kg/day), TB-500 (60 μg/kg/day), and combined BPC-157 + TB-500 (BPC + TB). Treatments were administered intraperitoneally for four weeks postoperatively. At four weeks, tendons were harvested for biomechanical testing or histological evaluation. Maximum load to failure was assessed biomechanically. Histological and histochemical analyses included hematoxylin-eosin, Masson trichrome, Alcian blue, and Sirius red staining and were evaluated using Bonar and Movin scoring systems. Expression of collagen types I and III was assessed immunohistochemically and semiquantified using H-score analysis.

Results: Biomechanical testing revealed higher maximum load to failure values in the BPC-157 and TB-500 groups compared to controls, reaching statistical significance in the TB-500 group ($p < 0.05$). Histopathological evaluation demonstrated significantly lower total Bonar scores in the TB-500 group ($p = 0.016$) and significantly lower total Movin scores in the TB-500 and BPC + TB groups ($p = 0.017$ and $p = 0.040$, respectively) relative to controls, indicating improved tendon architecture, collagen alignment, and reduced degenerative changes. The BPC-157 group showed numerically lower scores without reaching statistical significance for total scores. Sirius red birefringence analysis showed increased type I collagen organization and altered type III collagen distribution in treatment groups, particularly in the TB-500 group, suggesting progression toward matrix maturation. Immunohistochemical analysis revealed no significant differences in collagen type I expression among groups, whereas collagen type III expression differed significantly, consistent with histochemical findings. Combined BPC-157 and TB-500 treatment did not confer additional benefits compared to either agent alone.

Conclusion: In this exploratory rat model study, both BPC-157 and TB-500 were associated with improved histopathological parameters and extracellular matrix organization during early Achilles tendon repair, with TB-500 additionally demonstrating a significant biomechanical advantage at four weeks. The absence of additive effects with combination therapy may reflect convergence on shared downstream pathways; however, this hypothesis requires further experimental confirmation. These preliminary findings indicate that both peptides warrant further investigation as candidate adjuncts to tendon repair, pending dose-optimization and longer-term studies.

Keywords: Achilles tendon, angiogenesis, BPC-157, collagen remodeling, TB-500, tendon healing, thymosin beta-4.

functional recovery, biomechanical strength, and histological organization following Achilles tendon injury.[10,11] Experimental evidence further suggests that BPC-157 promotes tendon fibroblast migration, cell survival, and extracellular matrix remodeling, processes that are critical for effective tendon repair.[12-14] Collectively, these findings suggest that BPC-157 may positively influence tendon healing processes.

Thymosin beta-4 (Tβ4) is an endogenous peptide involved in angiogenesis, inflammatory regulation, cell migration, and extracellular matrix remodeling.[15-17] The TB-500 is a synthetic peptide derived from Tβ4 and was developed to mimic its regenerative properties.[18] Based on these biological properties, TB-500 has attracted interest as a potential therapeutic agent for tendon healing, particularly in tissues with limited vascularity and regenerative capacity. However, in contrast to BPC-157, experimental evidence supporting the role of TB-500 in tendon-specific healing remains scarce, and controlled studies in Achilles tendon injury models are largely absent from the literature. This knowledge gap provided a major rationale for the present study.

The present study was designed to build upon previous experimental findings regarding BPC-157 and to provide, to our knowledge, the first direct comparison of TB-500 and BPC-157 in a rat Achilles tendon rupture-repair model using standardized biomechanical, histopathological, histochemical, and immunohistochemical outcome measures. Since BPC-157 and TB-500 have been reported to affect different aspects of tissue repair, a combination treatment group was included to investigate whether concurrent administration could provide additive benefits during tendon healing.[7-9,14,19-21] Therefore, we hypothesized that concurrent administration would provide additive benefits during tendon healing. The aim of this study was to compare the effects of BPC-157, TB-500, and their combination on Achilles tendon healing in rats.

MATERIALS AND METHODS

The study was conducted and reported in accordance with the ARRIVE (Animal Research: Reporting of In Vivo Experiments) guidelines. This experimental study involved 32 young adult male Sprague-Dawley rats, each aged 12 weeks and weighing approximately 330 g. Following a 10-day acclimatization period, all animals were randomly allocated into four groups, with eight rats in each group, using a simple randomization procedure: control group, BPC-157 group , TB-500 group, and BPC-157 + TB-500 (BPC + TB) group. Within each group, tendons were allocated to specific analytical endpoints: four tendons per group were designated for biomechanical testing and four tendons per group were designated for histological processing, including Bonar and Movin histopathological scoring, Sirius red birefringence analysis, and immunohistochemical evaluation. Accordingly, the effective sample size for all nonbiomechanical analyses reported in this manuscript was n = 4 per group. Rats received daily intraperitoneal injections for 30 postoperative days according to group allocation (Figure 1). The control group received intraperitoneal vehicle administration, the BPC-157 group received BPC-157 at a dose of 10 μg/kg/day, the TB-500 group received TB-500 at a dose of 60 μg/kg/day, and the combination group received both BPC-157 (10 μg/kg/day) and TB-500 (60 μg/kg/day) via the intraperitoneal route.

Beginning on the first postoperative day, BPC-157 (223-018-PS; Peptide Sciences, Boca Raton, FL, USA) and TB-500 (27-155-PS; Peptide Sciences, Boca Raton, FL, USA) were administered once daily. The BPC-157 dose of 10 μg/kg/day was selected based on the established effective dose used in foundational preclinical tendon studies, in which this intraperitoneal regimen consistently produced significant functional, biomechanical, and histological improvements.[10,11] The TB-500 dose of 60 μg/kg/day was selected based on biologically active dose ranges reported for Tβ4 in preclinical soft tissue repair models employing systemic intraperitoneal administration.[16,17] It should be noted that formal dose-optimization studies for TB-500 in tendon-specific injury models are currently absent from the published literature; the selected dose, therefore, represents a biologically informed initial regimen, and dose-response characterization remains an important direction for future investigation.[22]

On day 30, all animals were sacrificed. No animal deaths, postoperative infections, wound complications, tendon reruptures, or protocol-related exclusions occurred during the study period. Therefore, all animals completed the study and were included in the final analyses according to their assigned groups. Of the eight animals per group, four tendons were randomly allocated to biomechanical testing and four to histological, histochemical, and immunohistochemical evaluation. Sample size for histological analyses (n = 4 tendons per group) was determined based

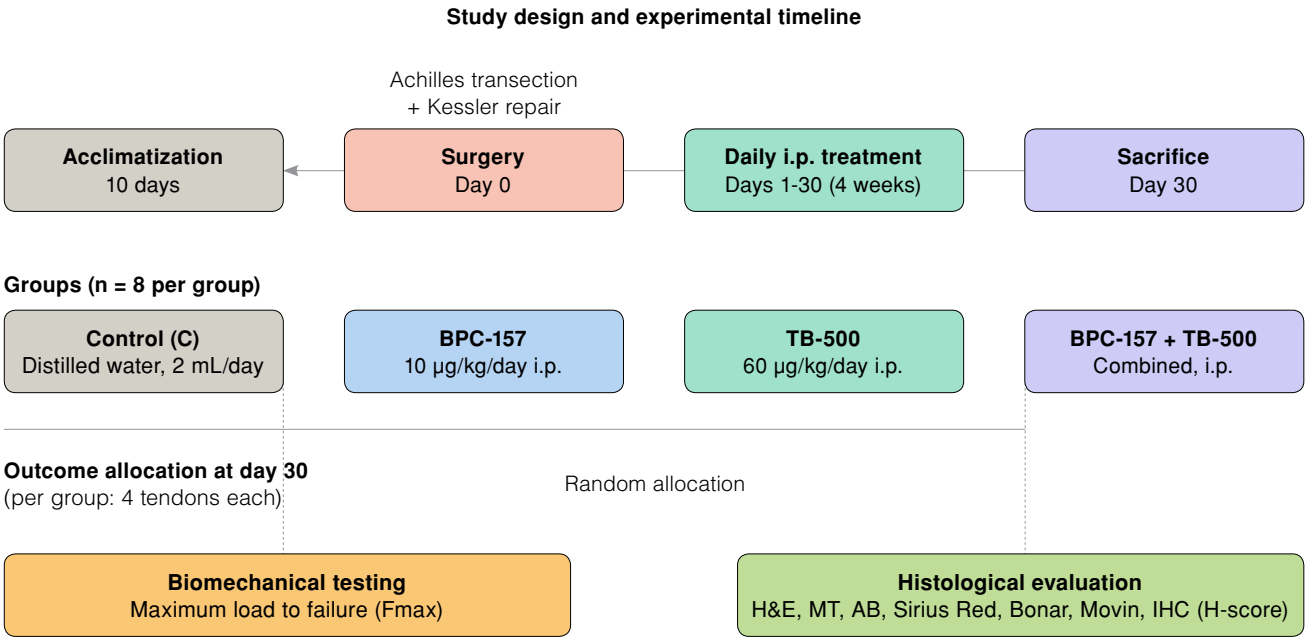


FIGURE 1. Schematic overview of the experimental design and treatment timeline. Sprague-Dawley rats (n = 32) underwent a 10-day acclimatization period prior to standardized Achilles tendon transection and primary Kessler repair (day 0). Animals were randomly allocated to four treatment groups (n = 8 per group) and received daily intraperitoneal injections for 30 days. At sacrifice (day 30), four tendons per group were randomly assigned to biomechanical testing and four to histological, histochemical, and immunohistochemical evaluation.

AB, Alcian blue; H&E, hematoxylin-eosin; IHC, immunohistochemistry; i.p., intraperitoneal; MT, Masson trichrome.

on the anticipated large effect sizes reported for histopathological scoring outcomes in comparable rodent tendon repair models. Post hoc power analysis confirmed achieved power ≥ 0.80 for 12 of 14 primary histological, histochemical, and immunohistochemical outcome variables (η^2 range: 0.41-0.94; Cohen's f range: 0.84-4.11; alpha = 0.05). Sample size for biomechanical testing (n = 4 tendons per group) was determined to provide adequate power for the detection of moderate-to-large differences in maximum load to failure, consistent with prior tendon biomechanical studies in this model.

Histopathological evaluation was performed by a pathologist blinded to group allocation. Histopathological scoring was performed within the tendon repair region on longitudinal sections. Scores were assigned based on representative microscopic areas reflecting the predominant morphological features of each specimen rather than on a single selected field. Biomechanical testing was conducted using coded specimens to ensure assessor blinding. Owing to the nature of the intervention, blinding was not feasible during surgical procedures or daily treatment administration. For immunohistochemical evaluation, stained sections were assessed within the tendon repair region using representative microscopic areas reflecting the predominant staining pattern of each specimen. Evaluations were performed under 10× and 20× magnification, corresponding to the magnifications used for representative image acquisition. Tendons designated for biomechanical assessment were stored at –20°C until testing, while those allocated to histological analysis were immediately fixed in 10% neutral buffered formalin.

Housing and husbandry

All animals were maintained in the experimental animal laboratory under standardized environmental circumstances, including a controlled temperature of 22 ± 2°C, relative humidity of 40-60%, and a 12-h light/dark cycle.[23] Standard pellet feed and tap water were provided ad libitum. Prior to the initiation of the study, rats underwent a 10-day acclimatization period. Following acclimatization, the animals were assigned to the groups and housed in separate cages, with four rats per cage and appropriate

identification labels. Body weights were monitored weekly throughout the four-week experimental duration.

Surgical procedure

A standardized Achilles tendon rupture and repair model was established, with all surgical procedures performed by the same surgeon to minimize interoperator variability. Each rat was weighed preoperatively to ensure accurate dose calculations. All animals received a single preoperative subcutaneous dose of gentamicin (8 mg/kg) for antimicrobial prophylaxis and were anesthetized with an intramuscular ketamine/xylazine combination (80/10 mg/kg). The right hind limb was shaved, disinfected with povidone-iodine (Batticon; Adeka, İstanbul, Türkiye), and draped under sterile conditions.

A 2-cm longitudinal incision was made along the posterior aspect of the right ankle to expose the Achilles tendon. A full transverse tenotomy was created 2 to 4 mm proximal to the calcaneal insertion using a No. 11 scalpel blade. Tendon repair was performed using the Kessler technique with 2-0 PDS sutures (DemeDiox; DemeTECH, Miami Lakes, FL, USA). The skin was subsequently closed with 2-0 silk sutures (Sterisilk; Yüce Tıbbi Gereçler A.Ş., İstanbul, Türkiye), and the incision site was cleansed with povidone-iodine.

Postoperative analgesia was provided with carprofen (3 mg/kg, Rimadyl; Pfizer, Manhattan, NY, USA) administered subcutaneously. Each rat was individually monitored for 24 h before being returned to its cage. Additional analgesia was administered every 12 h during the first postoperative day as needed. No immobilization or movement restriction was applied during the recovery period.

Histological, histochemical, immunohistochemical, and biomechanical analyses

Excised Achilles tendons, including both their proximal and distal attachment sites, were allocated for either histological or biomechanical evaluation. Samples designated for biomechanical testing were stored at −20°C until assessment. Mechanical testing was performed in the mechanical engineering laboratory using a 500-N electromechanical tensile testing device at a displacement rate of 1 mm/sec. Maximum load to failure (Fmax) and elongation values were digitally recorded.

For histological analysis, tendon specimens were fixed in 10% neutral buffered formalin, routinely processed, embedded in paraffin, and sectioned longitudinally at a thickness of 4 μm along the long axis of the tendon to allow assessment of fiber architecture, tenocyte morphology, and collagen organization across the full length of the repair site. Hematoxylin-eosin (H&E) staining was performed for general morphological evaluation. For histochemical assessment, serial sections mounted on positively charged slides were stained with Masson trichrome (MT) and Alcian blue (AB) using an automated histostainer, and evaluations were performed based on the Bonar and Movin scoring criteria.[24,25] Additional sections were stained with Sirius red as a histochemical method to evaluate collagen fiber organization and birefringence patterns under bright-field and polarized light microscopy. Separate sections were subjected to immunohistochemical staining for collagen type I using a mouse monoclonal anti-collagen type I antibody (COL1 [ABIN957814], 1:50; Antibodies-Online, Limerick, PA, USA) and for collagen type III using a rabbit polyclonal anti-collagen type III antibody (ab7778, 1:300; Abcam, Cambridge, UK).

All slides were examined under an Olympus CX51 microscope (Olympus Corp., Tokyo, Japan) by a single pathologist blinded to group assignments. Bonar scoring evaluated four parameters: tenocyte morphology/proliferation, ground substance (glycosaminoglycan [GAG]) content, collagen fiber alignment, and vascularity. Each parameter was rated on a scale from 0 (normal) to 3 (severely abnormal), producing a total score ranging from 0 to 12. Movin scoring included eight parameters: fiber structure, fiber arrangement, nuclear morphology, regional cellularity, increased vascularity, reduced collagen staining (MT), hyalinization, and GAG content (AB). Each item was scored 0-3, with a maximum total score of 24.

Immunohistochemical staining intensities for collagen type I and collagen type III were semiquantitatively assessed using the H-score method, which combines staining intensity and the percentage of positively stained tissue area to provide an integrated assessment of protein expression. The H-score was calculated as staining intensity × percentage of positive area (range 0-300), consistent with previously published tendon-healing studies.[26] Additionally, the polarization ratio, calculated as type I collagen/(type I collagen

+ type III collagen), was used as an indicator of relative tendon maturation.

Statistical analysis

Statistical analyses were conducted using GraphPad Prism version 8.1.1 (GraphPad Software, San Diego, CA, USA). Given that histological subgroups comprised four animals per group, formal normality testing (Kolmogorov-Smirnov) was considered to have insufficient statistical power to reliably detect departures from normality; accordingly, nonparametric methods were applied to all histological, histochemical, and immunohistochemical variables. The biomechanical data, histopathological scores (Bonar and Movin systems), histochemical data, and immunohistochemical variables (n = 4 per group) were reported as median (interquartile range,) and analyzed using the Kruskal-Wallis test. When a statistically significant overall difference was detected, pairwise comparisons were performed using Dunn's post hoc test with Bonferroni correction for multiple comparisons. Statistical significance was defined as $p < 0.05$.

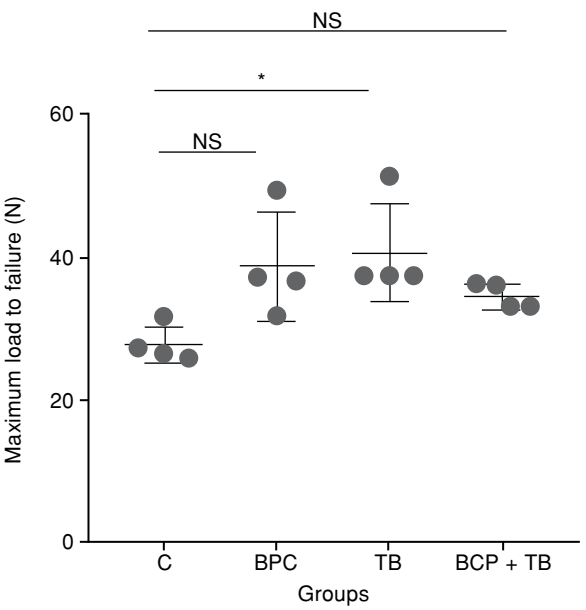


FIGURE 2. Maximum load to failure (Fmax) values in the control (C), BPC-157 (BPC), TB-500 (TB), and combined BPC + TB groups (n = 4 tendons per group; biomechanical testing cohort). Data are presented as median (IQR). Median [IQR] Fmax values were 26.91 [26.12-30.44] N for the C group, 37.16 [33.01-46.45] N for the BPC group, 37.41 [37.10-47.82] N for the TB group, and 34.54 [33.02-36.24] N for the BPC + TB group. Groups were compared using the Kruskal-Wallis test followed by Dunn's post hoc test for multiple comparisons.

IQR, interquartile range; * $p < 0.05$ versus the Control group (adjusted $p < 0.05$).

Ethical approval

All animal procedures were carried out in accordance with the National Guidelines for the Care and Use of Laboratory Animals and were fully compliant with EU Directive 2010/63/EU on the protection of animals used for scientific purposes. The study protocol was approved by the İstanbul Bağcılar Training and Research Hospital Animal Experiments Local Ethics Committee (Date: 15.06.2023, No: HADYEK/2023-12). All efforts were undertaken to minimize animal discomfort and to use the minimum number of animals necessary to achieve scientific validity.

RESULTS

Biomechanical analysis

Biomechanical testing revealed a significant overall difference in maximum load to failure (Fmax) among the groups (Kruskal-Wallis H = 7.712, $p = 0.0165$). Dunn's post hoc test showed that the only significant pairwise difference was between the TB-500 group and controls (adjusted $p = 0.0406$). The BPC-157 group did not differ significantly from controls (adjusted p = 0.389), and no other comparison reached significance (all adjusted $p > 0.999$). The combined BPC + TB group did not differ from any group (Figure 2).

Histological and histochemical evaluations

Histological analyses demonstrated differences in tendon architecture and extracellular matrix organization among the study groups (Figure 3). Control tendons exhibited disrupted architecture, increased cellularity, irregular tenocyte morphology, disorganized collagen bundles, and prominent GAG accumulation. In contrast, the treatment groups generally demonstrated more organized tissue architecture, reduced pathological cellularity, more uniform spindle-shaped tenocytes, improved collagen alignment, and reduced ground substance. These qualitative findings were particularly evident in the TB-500 group. The combined BPC + TB group demonstrated similar histological features without an obvious qualitative advantage over the individual treatment groups.

Significant intergroup differences were observed in tenocyte morphology/proliferation ($p = 0.004$), ground substance/GAG content ($p = 0.009$), collagen alignment ($p = 0.028$), and total Bonar score ($p = 0.005$; Table I). For total Bonar score, post hoc analysis

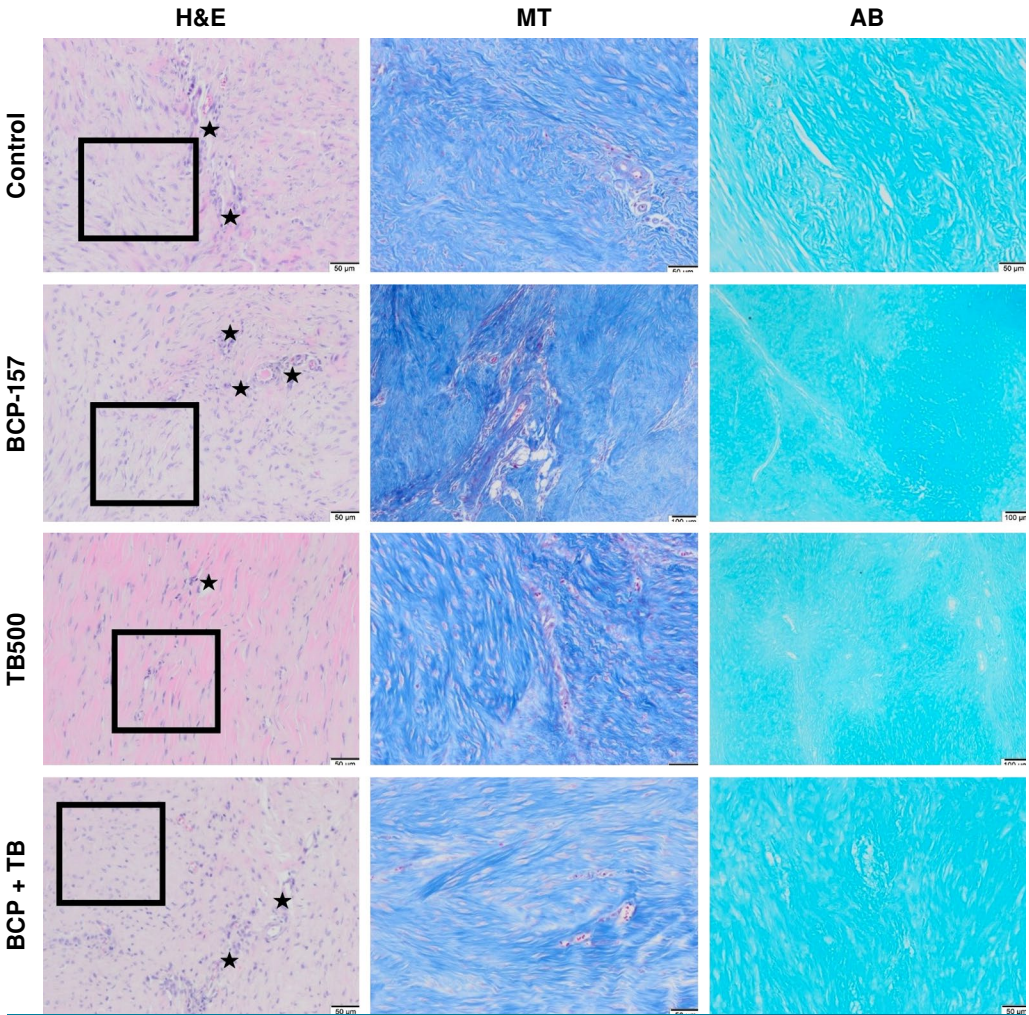


FIGURE 3. Representative histological and histochemical images of Achilles tendon healing (n = 4 tendons per group). Representative micrographs from the control, BPC-157, TB-500, and combined BPC + TB groups stained with H&E, MT, and AB. Square-marked areas in H&E images indicate representative regions of cellularity used for semiquantitative scoring and collagen bundle organization and alignment patterns. Asterisks (*) indicate vascular structures evaluated under the vascularity scoring criterion. Scale bars are indicated individually for each panel. For H&E, all groups are shown at 50 µm (×20 magnification). For MT panels, control and BPC + TB groups are shown at 50 µm (×20), while BPC-157 and TB-500 groups are shown at 100 µm (×10). For AB panels, control and BPC + TB groups are shown at 50 µm (×20), while BPC-157 and TB-500 groups are shown at 100 µm (×10). Histopathological scores were analyzed using the Kruskal-Wallis test followed by Dunn's post hoc test for multiple comparisons.
BPC, BPC-157; TB, TB-500; BPC + TB, combination; MT, Masson trichrome; AB, Alcian blue.

revealed a significant difference only between the control and TB-500 groups (p = 0.016); the BPC-157 (p = 0.273) and BPC + TB (p = 0.103) groups did not differ significantly from controls. The TB-500 and BPC + TB groups demonstrated significantly lower scores than controls for tenocyte morphology and ground substance. Collagen alignment differed significantly only between the control and TB-500 groups (p = 0.049). No significant differences were observed for vascularity (p = 0.108), and no significant differences were detected among the treatment groups for total Bonar score.

Alcian blue staining, evaluated according to the Movin scoring system (Figure 3), similarly demonstrated significant intergroup differences in fiber structure (p = 0.002), fiber arrangement (p = 0.007), nuclear morphology (p = 0.006), regional cellularity (p = 0.004), decreased collagen staining (p = 0.002), hyalinization (p = 0.040), GAG content

TABLE I

Bonar histopathological scoring

Variables	C		BPC		TB		BPC + TB		*p* (overall)	Post-hoc *p* values
	Median	IQR	Median	IQR	Median	IQR	Median	IQR		
Tenocyte morphology / proliferation (0-3)	2.5	2.0-3.0	1.5	1.0-2.0	1.0	1.0-1.0	1.0	1.0-1.0	**0.004**	C *vs.* BPC: 0.507 C *vs.* TB: 0.020* C *vs.* BPC + TB: 0.020* BPC *vs.* TB: > 0.999 BPC *vs.* BPC + TB: > 0.999 TB *vs.* BPC + TB: > 0.999
Ground substance / GAG (0-3)	2.0	2.0-2.75	1.0	1.0-1.75	1.0	1.0-1.0	1.0	1.0-1.0	**0.009**	C *vs.* BPC: 0.135 C *vs.* TB: 0.018* C *vs.* BPC + TB: 0.018* BPC *vs.* TB: > 0.999 BPC *vs.* BPC + TB: > 0.999 TB *vs.* BPC + TB: > 0.999
Collagen bundle alignment (0-3)	3.0	2.25-3.0	1.5	1.0-2.0	1.0	1.0-1.75	1.5	1.0-2.0	**0.028**	C *vs.* BPC: 0.203 C *vs.* TB: 0.049* C *vs.* BPC + TB: 0.203 BPC *vs.* TB: > 0.999 BPC *vs.* BPC + TB: > 0.999 TB *vs.* BPC + TB: > 0.999
Vascularity (0-3)	2.0	1.25-2.0	1.0	1.0-1.0	1.0	1.0-1.0	1.0	1.0-1.75	0.108	C *vs.* BPC: 0.106 C *vs.* TB: 0.106 C *vs.* BPC + TB: 0.683 BPC *vs.* TB: > 0.999 BPC *vs.* BPC + TB: > 0.999 TB *vs.* BPC + TB: > 0.999
Total Bonar (0-12)	9.5	7.5-10.75	5.0	4.25-5.75	4.0	4.0-4.75	4.5	4.25-5.75	**0.005**	C *vs.* BPC: 0.273 C *vs.* TB: 0.016* C *vs.* BPC + TB: 0.103 BPC *vs.* TB: > 0.999 BPC *vs.* BPC + TB: > 0.999 TB *vs.* BPC + TB: > 0.999

C, control; BPC, BPC-157; TB, TB-500; BPC + TB, combination; IQR, interquartile range; GAG, glycosaminoglycan. Kruskal-Wallis test with Dunn's post-hoc; n = 4 per group; * $p < 0.05$ indicate statistically significant pairwise comparisons.

TABLE II
Movin histopathological scoring

Variables	C		BPC		TB		BPC + TB		*p* (overall)	Post-hoc *p* values
	Median	IQR	Median	IQR	Median	IQR	Median	IQR		
Fiber structure (0-3)	3.0	2.25-3.0	1.5	1.0-2.0	1.0	1.0-1.0	1.0	1.0-1.0	0.002	C *vs.* BPC: 0.351 C *vs.* TB: 0.016* C *vs.* BPC + TB: 0.016* BPC *vs.* TB: > 0.999 BPC *vs.* BPC + TB: > 0.999 TB *vs.* BPC + TB: > 0.999
Fiber arrangement (0-3)	3.0	2.25-3.0	1.0	1.0-1.0	1.0	1.0-1.75	1.0	1.0-1.75	0.007	C *vs.* BPC: 0.016* C *vs.* TB: 0.086 C *vs.* BPC + TB: 0.086 BPC *vs.* TB: > 0.999 BPC *vs.* BPC + TB: > 0.999 TB *vs.* BPC + TB: > 0.999
Nuclear morphology (0-3)	2.0	2.0-2.75	1.5	1.0-2.0	1.0	1.0-1.0	1.0	1.0-1.0	0.006	C *vs.* BPC: 0.703 C *vs.* TB: 0.025* C *vs.* BPC + TB: 0.025* BPC *vs.* TB: > 0.999 BPC *vs.* BPC + TB: > 0.999 TB *vs.* BPC + TB: > 0.999
Regional cellularity (0-3)	2.5	2.0-3.0	1.5	1.0-2.0	1.0	1.0-1.0	1.0	1.0-1.0	0.004	C *vs.* BPC: 0.507 C *vs.* TB: 0.020* C *vs.* BPC + TB: 0.020* BPC *vs.* TB: > 0.999 BPC *vs.* BPC + TB: > 0.999 TB *vs.* BPC + TB: > 0.999
Increased vascularity (0-3)	2.0	1.25-2.0	1.0	1.0-1.0	1.0	1.0-1.0	1.0	1.0-1.0	0.029	C *vs.* BPC: 0.051 C *vs.* TB: 0.051 C *vs.* BPC + TB: 0.051 BPC *vs.* TB: > 0.999 BPC *vs.* BPC + TB: > 0.999 TB *vs.* BPC + TB: > 0.999
Decreased collagen staining (MT) (0-3)	2.0	2.0-2.0	1.0	1.0-1.0	1.0	0.25-1.0	1.0	1.0-1.0	0.002	C *vs.* BPC: 0.037* C *vs.* TB: 0.006** C *vs.* BPC + TB: 0.037* BPC *vs.* TB: > 0.999 BPC *vs.* BPC + TB: > 0.999 TB *vs.* BPC + TB: > 0.999

TABLE II
Continued

Variables	C		BPC		TB		BPC + TB		*p* (overall)	Post-hoc *p* values
	Median	IQR	Median	IQR	Median	IQR	Median	IQR		
Hyalinization (0-3)	1.5	1.0-2.0	1.0	1.0-1.0	1.0	1.0-1.0	0.5	0.0-1.0	0.040	C *vs.* BPC: > 0.999 C *vs.* TB: > 0.999 C *vs.* BPC + TB: 0.037* BPC *vs.* TB: > 0.999 BPC *vs.* BPC + TB: > 0.999 TB *vs.* BPC + TB: > 0.999
GAG content (AB) (0-3)	2.0	1.25-2.0	1.0	1.0-1.0	1.0	1.0-1.0	1.0	1.0-1.0	0.029	C *vs.* BPC: 0.051 C *vs.* TB: 0.051 C *vs.* BPC + TB: 0.051 BPC *vs.* TB: > 0.999 BPC *vs.* BPC + TB: > 0.999 TB *vs.* BPC + TB: > 0.999
Total Movin (0-24)	18.0	14.0-19.75	9.5	8.25-10.75	8.0	7.25-8.75	8.0	8.0-8.75	0.002	C *vs.* BPC: 0.601 C *vs.* TB: 0.017* C *vs.* BPC + TB: 0.040* BPC *vs.* TB: > 0.999 BPC *vs.* BPC + TB: > 0.999 TB *vs.* BPC + TB: > 0.999

C, control; BPC, BPC-157; TB, TB-500; BPC + TB, combination; IQR, interquartile range; MT, Masson trichrome; AB, Alcian blue; GAG, glycosaminoglycan. Kruskal-Wallis test with Dunn's post-hoc; n = 4 per group; * $p < 0.05$; ** $p < 0.01$ indicate statistically significant pairwise comparisons.

($p = 0.029$), and total Movin score ($p = 0.002$; Table II). For total Movin score, post hoc analysis revealed significant differences between controls and the TB-500 group ($p = 0.017$) and between controls and the BPC + TB group ($p = 0.040$); the BPC-157 group did not differ significantly from controls ($p = 0.601$). No statistically significant differences were observed among treatment groups.

Collagen characterization: Sirius red birefringence

Sirius red birefringence demonstrated differences in collagen fiber organization among the study groups (Figure 4). Control tendons exhibited a more heterogeneous birefringence pattern, whereas treatment groups generally demonstrated more uniform collagen fiber organization. Significant differences were observed in type I collagen intensity ($p < 0.001$), type III collagen intensity ($p < 0.001$), and polarization ratio ($p = 0.030$; Table III). Type I collagen intensity was higher in the BPC-157 ($p = 0.009$) and TB-500 ($p = 0.041$) groups compared to controls. Type III collagen intensity differed between the BPC-157 and TB-500 groups ($p = 0.028$). No consistent superiority was observed for combined treatment.

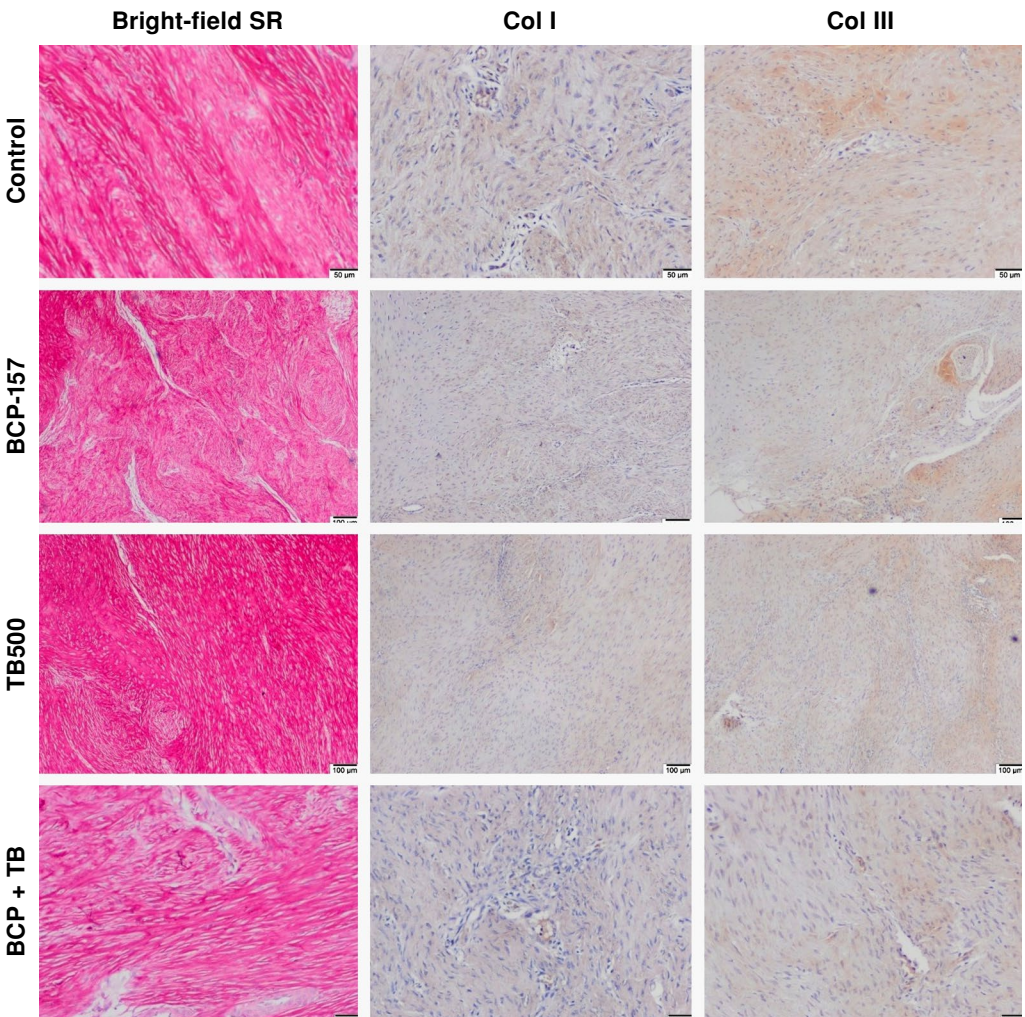


FIGURE 4. Sirius red birefringence and immunohistochemical evaluation of collagen composition during Achilles tendon healing (n = 4 tendons per group). Representative micrographs from the control, BPC-157, TB-500, and BPC + TB groups under bright-field Sirius red (SR) and immunohistochemical staining for collagen type I (COL I) and collagen type III (COL III). Scale bars are indicated individually for each panel. For all stains, the control and BPC + TB groups are shown at 50 µm (×20 magnification), whereas the BPC-157 and TB-500 groups are shown at 100 µm (×10). Sirius red birefringence and immunohistochemical data were analyzed using the Kruskal-Wallis test followed by Dunn's post hoc test for multiple comparisons.
BPC, BPC-157; TB, TB-500; BPC + TB, combination.

TABLE III
Sirius Red birefringence analysis

Variables	C		BPC		TB		BPC + TB		*p* (overall)	Post-hoc *p* values
	Median	IQR	Median	IQR	Median	IQR	Median	IQR		
Mean type I intensity (0-3)	1.0	1.0-1.0	3.0	2.25-3.0	2.5	2.0-3.0	2.0	2.0-2.0	< 0.001	C *vs.* BPC: 0.009** C *vs.* TB: 0.041* C *vs.* BPC + TB: 0.483 BPC *vs.* TB: > 0.999 BPC *vs.* BPC + TB: 0.916 TB *vs.* BPC + TB: > 0.999
Mean type III intensity (0-3)	2.0	2.0-2.0	1.0	1.0-1.0	2.0	2.0-2.75	1.0	1.0-1.0	< 0.001	C *vs.* BPC: 0.075 C *vs.* TB: > 0.999 C *vs.* BPC + TB: 0.075 BPC *vs.* TB: 0.028* BPC *vs.* BPC + TB: > 0.999 TB *vs.* BPC + TB: 0.028*
Polarization ratio = type I / (type I + type III)	0.33	0.33-0.33	0.73	0.36-0.75	0.50	0.50-0.58	0.29	0.27-0.32	0.030	C *vs.* BPC: > 0.999 C *vs.* TB: > 0.999 C *vs.* BPC + TB: > 0.999 BPC *vs.* TB: > 0.999 BPC *vs.* BPC + TB: 0.098 TB *vs.* BPC + TB: 0.098

C, control; BPC, BPC-157; TB, TB-500; BPC + TB, combination; IQR, interquartile range; Kruskal-Wallis test with Dunn's post-hoc; n = 4 per group; * $p < 0.05$; ** $p < 0.01$ indicate statistically significant pairwise comparisons.

TABLE IV
Immunohistochemical expression (H-Score)

Variables	C		BPC		TB		BPC + TB		*p* (overall)	Post-hoc *p* values
	Median	IQR	Median	IQR	Median	IQR	Median	IQR		
Collagen type I (H-Score, 0-300)	20.0	15.0-20.0	25.0	20.0-50.0	60.0	15.0-75.0	42.5	38.5-48.75	0.242	C *vs.* BPC: > 0.999 C *vs.* TB: 0.434 C *vs.* BPC + TB: 0.386 BPC *vs.* TB: > 0.999 BPC *vs.* BPC + TB: > 0.999 TB *vs.* BPC + TB: 0.208
Collagen type III (H-Score, 0-300)	12.5	10.0-15.0	10.0	6.25-10.0	72.5	40.0-116.25	37.5	33.5-41.5	< 0.001	C *vs.* BPC: > 0.999 C *vs.* TB: 0.093 C *vs.* BPC + TB: 0.576 BPC *vs.* TB: 0.009* BPC *vs.* BPC + TB: 0.093 TB *vs.* BPC + TB: > 0.999

C, control; BPC, BPC-157; TB, TB-500; BPC + TB, combination; IQR, interquartile range; H-Score, histochemical score (Intensity × % Area, range 0-300); Kruskal-Wallis test with Dunn's post-hoc; n = 4 per group unless noted; * $p < 0.01$ indicate statistically significant pairwise comparisons.

Immunohistochemical analysis

Immunohistochemical analysis demonstrated differences in collagen staining patterns among the study groups (Figure 4). Collagen type III distribution appeared to vary among groups, particularly in the TB-500 group, consistent with the H-score analysis. The combined treatment group exhibited a staining pattern comparable to that observed in the BPC-157 group.

No significant difference was detected in collagen type I expression ($p = 0.242$; Table IV). In contrast, collagen type III expression differed significantly among groups ($p < 0.0001$), with a significant difference observed between the BPC-157 and TB-500 groups ($p < 0.001$). No other pairwise comparisons reached statistical significance.

DISCUSSION

Tendon healing involves sequential inflammatory, proliferative, and remodeling phases characterized by progressive collagen organization and mechanical strengthening.[13] The Achilles tendon's relative hypovascularity predisposes it to delayed repair and inferior matrix maturation.[27,28] Therapies that enhance angiogenesis, matrix organization, and inflammatory regulation may therefore improve healing outcomes. In the present study, TB-500 was associated with significantly lower histopathological scores and higher maximum load to failure values compared to untreated controls, whereas BPC-157 improved selected histopathological parameters without significant reductions in total composite scores. These findings extend previous preclinical observations regarding BPC-157 and provide the first controlled comparison of TB-500 and BPC-157 in a surgically repaired Achilles tendon model using standardized biomechanical and histopathological outcome measures.

Previous studies using BPC-157 in rat Achilles tendon models have reported improvements in functional, biomechanical, and histological outcomes.[29] Staresinic et al.[10] demonstrated increased load to failure, Young's modulus, and Achilles Functional Index values following BPC-157 treatment in an unrepaired tendon transection model, whereas Krivic et al.[11] reported improved tendon-to-bone healing and collagen organization in an Achilles tendon detachment model. In contrast, all tendons in the present study underwent immediate primary repair using the Kessler technique, and

outcome assessment was performed only at four weeks postoperatively. These methodological differences may explain why BPC-157 was associated with improvements in selected histopathological parameters but did not significantly increase maximum load to failure. Accordingly, direct comparison of biomechanical outcomes across different experimental tendon-healing models should be interpreted with caution.

The BPC-157 possesses documented proangiogenic and cytoprotective properties mediated through vascular endothelial growth factor receptor 2 and Akt (protein kinase B)/eNOS (endothelial nitric oxide synthase) signaling pathways.[9,13,27,29,30] In the present study, BPC-157 improved selected histopathological parameters, including fiber arrangement and collagen staining, but did not significantly reduce total Bonar or Movin scores relative to controls. These findings are partially consistent with previous experimental studies demonstrating beneficial effects of BPC-157 on tendon healing.[10,11] However, unlike earlier models that used unrepaired tendon injuries and shorter follow-up periods, all tendons in the present study underwent primary repair and were evaluated at four weeks postoperatively. These methodological differences may explain the absence of a significant increase in maximum load to failure despite improvements in selected histological parameters.

The TB-500 was associated with improvements in both histopathological findings and maximum load to failure at four weeks. Treated tendons demonstrated better collagen alignment and lower GAG content than controls, findings that may be consistent with more advanced tissue organization.[19-22] In addition, the TB-500 group exhibited significantly higher maximum load to failure values than controls. Given the limited tendon-specific literature available for TB-500, these findings provide preliminary evidence supporting further investigation of this peptide in tendon-healing models. However, because biomechanical evaluation was limited to maximum load to failure, broader conclusions regarding overall mechanical performance should be interpreted with caution.

Collagen composition is central to tendon healing and mechanical function. Healing is characterized by early collagen type III deposition followed by gradual transition toward a collagen type I-dominant extracellular matrix.[31-33] In the present study, treatment groups demonstrated enhanced collagen type I birefringence and altered collagen type III distribution, findings that may reflect ongoing matrix remodeling.[4,34,35] Similar observations have been reported in previous BPC-157 musculoskeletal models. Cerovecki et al.[12] demonstrated accelerated replacement of collagen type III with type I fibers following medial collateral ligament transection, while Krivic et al.[11] reported altered collagen organization in BPC-157-treated Achilles tendon detachment specimens. In the present study, Sirius red birefringence analysis demonstrated differences in collagen organization among the treatment groups, particularly in the TB-500 group. However, no significant difference in collagen type I H-score was detected, suggesting that birefringence findings may primarily reflect collagen fiber alignment and organization rather than increased collagen synthesis. Accordingly, these findings should be interpreted as evidence of matrix remodeling rather than definitive proof of enhanced tendon maturation.

The significantly elevated collagen type III H-score observed in the TB-500 group warrants careful interpretation and should not be assumed to reflect unequivocally favorable repair. Increased collagen type III deposition is a recognized feature of the proliferative phase of tendon healing and typically precedes the gradual restoration of a collagen type I-dominant extracellular matrix.[4,31,32,34] Therefore, the increased collagen type III expression observed at four weeks should be interpreted within the temporal context of tendon repair and may reflect active matrix remodeling rather than pathological fibrosis. In the present study, elevated collagen type III expression in the TB-500 group was accompanied by improved Bonar and Movin scores, reduced GAG accumulation, enhanced collagen type I birefringence, and higher maximum load to failure values compared to controls. Taken together, these findings suggest that the increased collagen type III expression may reflect an active remodeling process rather than aberrant scar formation. Nevertheless, assessment at later time points and molecular analyses of collagen turnover pathways are required to determine whether TB-500 ultimately promotes regenerative matrix maturation or scar-mediated repair.

The absence of additive effects with combined BPC-157 and TB-500 administration represents an important finding of the present study. Although the two peptides have been proposed to influence tendon healing through distinct biological pathways,[14,19,29] combined treatment

did not demonstrate superior biomechanical or histopathological outcomes compared to monotherapy. Several hypothetical explanations may account for this observation, including overlapping downstream effects, ceiling effects during the early remodeling phase, or suboptimal combination dosing strategies. However, because no molecular or pharmacokinetic analyses were performed, the mechanisms underlying the lack of additive benefit remain speculative. Further studies incorporating multiple time points, molecular analyses, and pharmacokinetic investigations will be required to experimentally verify these hypotheses and to clarify whether alternative dosing regimens or treatment schedules influence the interaction between these peptides.

Several limitations of the present study warrant consideration. First, outcome assessment was performed at a single time point (four weeks after repair), which captured only the early proliferative-to-remodeling transition and did not allow characterization of later-stage tendon maturation. Second, the use of healthy young male rats may limit generalizability to clinical populations with comorbidities known to impair tendon healing. Third, no functional assessment was performed, limiting direct comparison with previous tendon-healing studies and reducing translational interpretation. Fourth, no molecular analyses were conducted; therefore, mechanistic explanations regarding the biological actions of BPC-157 and TB-500 remain speculative. Fifth, the TB-500 dose was selected from the broader Tβ4 literature rather than from tendon-specific dose-optimization studies. Sixth, histological analyses were performed on a subset of animals (n = 4 per group), and a prospective a priori power calculation was not performed. In addition, interobserver reliability was not assessed, and blinding was not feasible during surgical procedures or daily treatment administration. Finally, tendon cross-sectional area was not measured, precluding calculation of stress-based biomechanical parameters such as ultimate tensile stress and Young's modulus. Biomechanical evaluation was further limited to maximum load to failure and did not include complementary parameters such as stiffness, energy to failure, or failure mode analysis. Therefore, the present findings should be interpreted as preliminary and require confirmation in larger studies incorporating longitudinal, functional, molecular, and more comprehensive biomechanical assessments.

Overall, the present findings suggest that peptide-based modulation of tendon repair warrants further investigation. At four weeks, TB-500 was associated with higher maximum load to failure values, whereas BPC-157 demonstrated improvements in selected histopathological parameters. Achilles tendon rupture remains a common and functionally significant injury, and current treatment strategies do not consistently restore native tendon properties during the early phases of healing. In this context, the observation that TB-500 was associated with increased maximum load to failure may justify further preclinical evaluation in tendon-healing models. However, no clinical data currently exist for either agent in tendon-specific applications, and direct extrapolation from healthy young rat models to human populations should be approached with caution. Additional preclinical studies incorporating multiple time points, functional outcomes, and comprehensive biomechanical assessments are required before clinical investigation can be considered.

In conclusion, this exploratory study provides preliminary evidence that both BPC-157 and TB-500 may improve histopathological organization and extracellular matrix remodeling during early Achilles tendon repair in a rat rupture-repair model. Additionally, TB-500 demonstrated significantly higher maximum load to failure values at four weeks. These findings are consistent with the broader preclinical literature on peptide-mediated connective tissue repair and suggest that both agents merit further systematic evaluation. However, given the single time point assessment, the use of a healthy young rat model, and the absence of formal dose-response characterization, particularly for TB-500, these results should be regarded as hypothesis-generating rather than confirmatory. Large preclinical studies incorporating multiple sacrifice time points, functional outcome measures, molecular pathway analyses, dose-response designs, and clinically relevant animal models of compromised healing are needed before the translational potential of these agents can be meaningfully assessed in clinical investigations.

Data Sharing Statement: The data that support the findings of this study are available from the corresponding author upon reasonable request.

Author Contributions: O.A, O.B.: Idea/concept, control/supervision; O.A., O.B., Y.G.: Design; E.C.B., Y.M.D.: Data collection and/or processing; B.Y.B.: Analysis and/or interpretation; B.Y.B., M.Y.Y., C.A.: Literature review;

O.B., Y.G..: Writing the article; M.Y.Y., C.A.: Critical review, references and fundings; O.A., O.B., E.C.B., Y.M.D., M.Y.Y., C.A., Y.G., B.Y.B.: Materials.

Conflict of Interest: The authors declared no conflicts of interest with respect to the authorship and/or publication of this article.

Funding: The authors received no financial support for the research and/or authorship of this article.

AI Disclosure: The authors declare that artificial intelligence (AI) tools were not used, or were used solely for language editing, and had no role in data analysis, interpretation, or the formulation of conclusions. All scientific content, data interpretation, and conclusions are the sole responsibility of the authors. The authors further confirm that AI tools were not used to generate, fabricate, or 'hallucinate' references, and that all references have been carefully verified for accuracy.

REFERENCES

1. Hammerman M, Pierantoni M, Isaksson H, Eliasson P. Deprivation of loading during rat Achilles tendon healing affects extracellular matrix composition and structure, and reduces cell density and alignment. Sci Rep 2024;14:23380. doi: 10.1038/s41598-024-74783-w.
2. Holm C, Kjaer M, Eliasson P. Achilles tendon rupture--treatment and complications: A systematic review. Scand J Med Sci Sports 2015;25:e1-10. doi: 10.1111/sms.12209.
3. Ocak M, Yilmaz S, Çam SB, Bilecenoğlu B, Dönmez BÖ, Korkusuz P, et al. Computed microtomographic imaging of revascularization during healing of Achilles tendon injury. J Anat 2025;247:363-74. doi: 10.1111/joa.14249.
4. Schulze-Tanzil GG, Delgado-Calcares M, Stange R, Wildemann B, Docheva D. Tendon healing: A concise review on cellular and molecular mechanisms with a particular focus on the Achilles tendon. Bone Joint Res 2022;11:561-74. doi: 10.1302/2046-3758.118.BJR-2021-0576.R1.
5. Szergyuk I, Del Carmen Yika A, Walocha JA, Pękala PA. The twisted Achilles tendon microvasculature. Folia Morphol (Warsz) 2024;83:565-70. doi: 10.5603/fm.98393.
6. Józwiak M, Bauer M, Kamysz W, Kleczkowska P. Multifunctionality and possible medical application of the BPC 157 peptide-literature and patent review. Pharmaceuticals (Basel) 2025;18:185. doi: 10.3390/ph18020185.
7. Seiwerth S, Rucman R, Turkovic B, Sever M, Klicek R, Radic B, et al. BPC 157 and standard angiogenic growth factors. Gastrointestinal tract healing, lessons from tendon, ligament, muscle and bone healing. Curr Pharm Des 2018;24:1972-89. doi: 10.2174/1381612824666180712110447.
8. Gwyer D, Wragg NM, Wilson SL. Gastric pentadecapeptide body protection compound BPC 157 and its role in accelerating musculoskeletal soft tissue healing. Cell Tissue Res 2019;377:153-9. doi: 10.1007/s00441-019-03016-8.
9. McGuire FP, Martinez R, Lenz A, Skinner L, Cushman DM. Regeneration or risk? A narrative review of BPC-157 for musculoskeletal healing. Curr Rev Musculoskelet Med 2025;18:611-9. doi: 10.1007/s12178-025-09990-7.
10. Staresinic M, Sebecic B, Patrlj L, Jadrijevic S, Suknaic S, Perovic D, et al. Gastric pentadecapeptide BPC 157 accelerates healing of transected rat Achilles tendon and in vitro stimulates tendocytes growth. J Orthop Res 2003;21:976-83. doi: 10.1016/S0736-0266(03)00110-4.
11. Krivic A, Anic T, Seiwerth S, Huljev D, Sikiric P. Achilles detachment in rat and stable gastric pentadecapeptide BPC 157: Promoted tendon-to-bone healing and opposed corticosteroid aggravation. J Orthop Res 2006;24:982-9. doi: 10.1002/jor.20096.
12. Cerovecki T, Bojanic I, Brcic L, Radic B, Vukoja I, Seiwerth S, et al. Pentadecapeptide BPC 157 (PL 14736) improves ligament healing in the rat. J Orthop Res 2010;28:1155-61. doi: 10.1002/jor.21107.
13. Chartier C, ElHawary H, Baradaran A, Vorstenbosch J, Xu L, Efanov JI. Tendon: Principles of healing and repair. Semin Plast Surg 2021;35:211-5. doi: 10.1055/s-0041-1731632.
14. Chang CH, Tsai WC, Lin MS, Hsu YH, Pang JH. The promoting effect of pentadecapeptide BPC 157 on tendon healing involves tendon outgrowth, cell survival, and cell migration. J Appl Physiol (1985) 2011;110:774-80. doi: 10.1152/japplphysiol.00945.2010.
15. Zhang J, Long M, Sun Z, Yang C, Jiang X, He L, et al. Association between Thymosin beta-4, acute kidney injury, and mortality in patients with sepsis: An observational cohort study. Int Immunopharmacol 2021;101:108167. doi: 10.1016/j.intimp.2021.108167.
16. Malinda KM, Sidhu GS, Mani H, Banaudha K, Maheshwari RK, Goldstein AL, et al. Thymosin beta4 accelerates wound healing. J Invest Dermatol 1999;113:364-8. doi: 10.1046/j.1523-1747.1999.00708.x.
17. Aksu U, Yaman OM, Guner I, Guntas G, Sonmez F, Tanriverdi G, et al. The protective effects of thymosin-β-4 in a rat model of ischemic acute kidney injury. J Invest Surg 2021;34:601-9. doi: 10.1080/08941939.2019.1672841.
18. Ho EN, Kwok WH, Lau MY, Wong AS, Wan TS, Lam KK, et al. Doping control analysis of TB-500, a synthetic version of an active region of thymosin β_4, in equine urine and plasma by liquid chromatography-mass spectrometry. J Chromatogr A 2012;1265:57-69. doi: 10.1016/j.chroma.2012.09.043.
19. Xing Y, Ye Y, Zuo H, Li Y. Progress on the function and application of thymosin β4. Front Endocrinol (Lausanne) 2021;12:767785. doi: 10.3389/fendo.2021.767785.
20. Ehrlich HP, Hazard SW 3rd. Thymosin beta4 enhances repair by organizing connective tissue and preventing the appearance of myofibroblasts. Ann N Y Acad Sci 2010;1194:118-24. doi: 10.1111/j.1749-6632.2010.05483.x.
21. Goldstein AL, Hannappel E, Sosne G, Kleinman HK. Thymosin β4: A multi-functional regenerative peptide. Basic properties and clinical applications. Expert Opin Biol Ther 2012;12:37-51. doi: 10.1517/14712598.2012.634793.
22. Philp D, Kleinman HK. Animal studies with thymosin beta, a multifunctional tissue repair and regeneration peptide. Ann N Y Acad Sci 2010;1194:81-6. doi: 10.1111/j.1749-6632.2010.05479.x.
23. Yildirim B, Erturk C, Buyukdogan H, Saritas TB, Yildirim Erdogan N, Ertem F. Effect of N-acetylcysteine on fracture healing in rat femoral diaphysis: A histopathological, radiological, and biomechanical analysis. Jt Dis Relat Surg 2025;36:283-92. doi: 10.52312/jdrs.2025.1975.
24. Khan KM, Cook JL, Bonar F, Harcourt P, Astrom M. Histopathology of common tendinopathies. Update and implications for clinical management. Sports Med 1999;27:393-408. doi: 10.2165/00007256-199927060-00004.
25. Movin T, Gad A, Reinholt FP, Rolf C. Tendon pathology in long-standing achillodynia. Biopsy findings in 40 patients. Acta Orthop Scand 1997;68:170-5. doi: 10.3109/17453679709004002.

26. Büyükdoğan H, Ertürk C, Eren E, Öztürk Ç, Yıldırım B, Sarıtaş TB, et al. The impact of N-acetylcysteine on early periods of tendon healing: Histopathologic, immunohistochemical, and biomechanical analysis in a rat model. Connect Tissue Res 2025;66:161-74. doi: 10.1080/03008207.2025.2479501.
27. Mansfield K, Dopke K, Koroneos Z, Bonaddio V, Adeyemo A, Aynardi M. Achilles tendon ruptures and repair in athletes-a review of sports-related achilles injuries and return to play. Curr Rev Musculoskelet Med 2022;15:353-61. doi: 10.1007/s12178-022-09774-3.
28. Pisano A, Caruso G. Direct anatomical reconstruction of the Achilles tendon and its application for surgical treatment of acute Achilles tendon ruptures; Surg Tech Dev 2024;13;382-92.
29. Vasireddi N, Hahamyan H, Salata MJ, Karns M, Calcei JG, Voos JE, et al. Emerging use of BPC-157 in orthopaedic sports medicine: A systematic review. HSS J 2025;21:15563316251355551. doi: 10.1177/15563316251355551.
30. Matek D, Jandrić M, Sikirić B, Oroz I, Sikirić P, Seiwerth S, et al. BPC 157 in musculoskeletal and junctional healing: Tendon, ligament, muscle, bone, and their junctions. Pharmaceuticals 2026;19:309.
31. Jiang L, Lu J, Chen Y, Lyu K, Long L, Wang X, et al. Mesenchymal stem cells: An efficient cell therapy for tendon repair (Review). Int J Mol Med 2023;52:70. doi: 10.3892/ijmm.2023.5273.
32. Kwan KYC, Ng KWK, Rao Y, Zhu C, Qi S, Tuan RS, et al. Effect of aging on tendon biology, biomechanics and implications for treatment approaches. Int J Mol Sci 2023;24:15183. doi: 10.3390/ijms242015183.
33. Gögele C, Pattappa G, Tempfer H, Docheva D, Schulze-Tanzil G. Tendon mechanobiology in the context of tendon biofabrication. Front Bioeng Biotechnol 2025;13:1560025. doi: 10.3389/fbioe.2025.1560025.
34. Leong NL, Kator JL, Clemens TL, James A, Enamoto-Iwamoto M, Jiang J. Tendon and ligament healing and current approaches to tendon and ligament regeneration. J Orthop Res 2020;38:7-12. doi: 10.1002/jor.24475.
35. DiIorio SE, Young B, Parker JB, Griffin MF, Longaker MT. Understanding tendon fibroblast biology and heterogeneity. Biomedicines 2024;12:859. doi: 10.3390/biomedicines12040859.